

Preliminary study of the point cloud obtained with a low cost structured light scanner of third lower human molars

Matteo Orsi^{1,3}, Nicol Rossetti², Roberto Taglioretti³, Silvia Zito⁴, Alessandra Mazzucchi^{5,3}

¹Department of Cultural and Environmental Heritage, University of Milan, 20142, Milan, Italy; ²Department of Biotechnology and Life Science, University of Insubria, Varese, Italy; ³LabDig 3A Academy Association; ⁴Independent researcher; ⁵Department of Cultural Heritage, University of Padua

Abstract. This study presents a preliminary exploration of an objective, operator-independent method for acquiring and analyzing point cloud data from human lower third molars using low-cost equipment. Emphasizing the need for affordability in the field, this research begins the development of a technical protocol for the validation and use of the structured light scanner EinScan-SP V1. Two human mandibular third molars from the crypt of Santa Maria Maggiore in Vercelli (Italy) are digitized. The teeth were scanned, and the resulting point clouds were processed using the Open3D library to extract and normalize digital indexes at different voxel levels. This work also introduces the concept of the Digital HyperUranium (IUD), a digital environment inspired by Platonic philosophy, to contextualize the mathematical processing of point clouds. The ultimate goal is to correlate digital indexes with biological profiles, enhancing the documentation and analysis of Cultural Heritage artifacts through affordable and automated digital acquisition methods.

Key words: structured light, point cloud, human teeth, protocol, new digital index

Introduction

This preliminary work is part of a wider project which has its focus on finding an objective way to obtain data from a point cloud. For the aim of this project, objective signifies the absence of intervention and influence of the operator on the process: in a digital context, this means that in the process of gathering data the operator does not directly act on the digital twin of the object to be investigated. The process is instead performed automatically by the execution of an algorithm.

The obvious premise of this project is the digital acquire of the point cloud. The digital acquire poses a problem in the field of Cultural Heritage, where the lack of resources does not consent an extensive and daily application of scanning techniques involving high cost instrumentation. For this reason, a key point is the validation and verification of low cost equipment,

meaning instrumentation costing less than 3000 €. The counterpart of the use of low cost instrumentation is, however, the absence of technical support for specific application fields such as anthropology or archaeology. This fact states the need for the development of technical protocols for the verification and the use of this equipment. The use of low cost instrumentation with the aid of specifically designed technical protocols can potentially accelerate the documentation process, allowing to gather better data in terms of accuracy, precision and quantity.

This is another founding core of the preliminary work presented here: a first attempt to apply these principles on two human mandibular third molars from the hypogeal cemetery of the Church of Santa Maria Maggiore in Vercelli (Piedmont, northern Italy) is evaluated in this work. The 3D scanning is performed with the low cost desktop structured light scanner EinScan-SP V1. The tooth was measured with

a digital caliper, whereas the point cloud is processed with the library Open3D (Zhou et al., 2018). The ultimate goal of the research is to identify possible correlations between the digital indexes obtained from the point cloud and the biological profile of the tooth owner, as well as between the physical measure and the biological profile.

Digital acquire is by now a well established practice in different fields: metrology and manufacturing, precision engineering, remote sensing, applied sciences. This practice has assumed an important role also in archaeology and anthropology. Widely applied techniques include photogrammetry (Evgenikou & Georgopoulos, 2015; Kusuma Frisky et al., 2020; Menna et al., 2016; Morena et al., 2019; Russo & Senatore, 2022), laser scanning (Bastir et al., 2019; Evgenikou & Georgopoulos, 2015; Garashchenko et al., 2022; Menna et al., 2016) and structured light scanning both with high cost equipment (Bastir et al., 2019; Diara, 2023; Garashchenko et al., 2022; Georgopoulos et al., 2016; Morena et al., 2019; Russo & Senatore, 2022) and entry-level to middle price equipment (Garashchenko et al., 2022; Kusuma Frisky et al., 2020; Maté-González et al., 2017). However, these scanners do not have suitable technical characteristics for our case.

It is worth to note that many of these works use different digital acquire techniques to compare the results in terms of distance, mean and root mean square error. Differently, Menna and colleagues (Menna et al., 2016), in the same way as Balletti and colleagues (Balletti et al., 2019), use a cooperative data fusion approach to integrate laser scanner and photogrammetry data: an approach which is well consolidate in engineering (Colosimo et al., 2015). These authors also highlight the need of a strong awareness of the technical and critical steps for the 3D acquisition, as well as the necessity of a correct planning and the high technical skills required to obtain quality models with photogrammetry.

Significantly, Williams and colleagues (Williams et al., 2024) report the limited “guidance and recommendations for 3D scanning procedures [...], resulting in the absence of standardisation across 3D specialists, professionals and beginners” in the field of archaeology. However, the aim to provide non-technical methodological pipelines stated by the authors is, in our

view, founded on the development of solid and verified technical protocols, which we are currently developing.

With a slightly different point of view, Jacobs and colleagues (Jacobs et al., 2023) perform a repeatability and reproducibility analysis of a specific desktop structured light scanner on a standard object. Different angles and different positions are tested systematically and quantitatively evaluated. A similar approach can be used to assess the same parameters for the EinScan-SP V1 structured light scanner.

Less practicable in the context of Cultural Heritage, but anyway worth mentioning, is the method applied by Dickin (Dickin et al., 2021) and Colosimo (Colosimo et al., 2015) to map and correct the local distortion intrinsic to the structured light scanning. Both of them use a mathematical approach and a CMM (Coordinate Measurement Machine) as higher accuracy reference to perform the correction.

The problem of gathering data from a digital acquire in the field of anthropology is addressed by the VA (Virtual Anthropology). This area of research mainly deals with functional morphology of hominids, as it is conceived by Gerhard W. Weber (Weber, 2014), through the use of different scanning techniques ranging from CT to structured light. The digital acquire can be processed with different algorithms, most of them applied in the context of GM (Geometric Morphometrics). GM involves the use of landmarks and semi-landmarks to perform a statistical analysis aimed to the quantitative comparison of object geometry. Weber also highlights that the aim of VA is to minimize the subjectivity of the entire process.

However, there is nor discussion neither conceptualization of how the environment in which the operations aimed to gather data from 3D objects, and particularly point clouds, works or should work. This void can potentially bring to confusion and misunderstanding about what the process of extracting data from point cloud implies. In order to fill this gap, we defined a new concept to define, describe and understand this environment. This digital environment is called IUD (IperUranio Digitale).

The IUD is a Euclidean space with 3 dimensions inspired from the Hyperuranium of the Greek philosopher Plato, populated only by points. Each point is defined by three Float64 numbers. These triplets

of Float64 numbers can be processed to obtain other sequences of Float64 numbers, expressing different characteristics of the point cloud. The software *os-teo_labdig* (*Labdig3a/Osteo_labdig: Digital Laboratory for Osteological Measurements*, n.d.) is used as a user interface to interact with the IUD with an anthropological perspective and it is used to load the point clouds in it. The tool shows a resizable window with a menu that permits a form of interaction with the point cloud loaded and an area to read the indexes calculated on it.

This software has an EUPL 1.2 license and can be modified to improve it to return the enhancements to the building community.

Defining this digital space, we thought of the well-known term from platonic philosophy “Hyperuranium”. This space is equipped with particular characteristics that make it “atopic”, far from any spatial form known in our physical universe: it is in fact a digital environment, reachable from our reality only through the physical mediation of a screen. It is multidimensional, containing floating objects that come from our reality, but which, in the new environment, become immaterial while remaining absolutely concrete at the same time; these are generated by means of mathematical formulas, a characteristic which makes them “perfect objects”. Lacking a specific term to connote a space which in fact is a “not-space”, at least according to our empirical experience, we therefore turned our attention to the ancient world: Plato, in the *Phaedrus* (Plato, *Phaedr.*, 247c–248c), offers us a definition of his Hyperuranium, a space similar to the environment we are attempting to conceptualize. A place “beyond the sky”, meaning not the physical place, but a reality that goes beyond the material space we know, in which the *psyché* (*ψυχή/soul*), the representation of what for Plato is the instrument of knowledge, learns in a new way, since the elements contained therein are not sensitive. The objects found in this non-place are characterized by the *ousia* (*οὐσία/essence*), perceivable only through the *nous* (*νοῦς/intellect*). For this reason, although the motivations behind this research and the aims of the well-known philosopher move in different directions, we wanted to call this environment “Digital Hyper Uranium”, thus wanting to trace a *fil rouge* that reaches us from the ancient world characterized by the use of knowledge as an absolute value of research.

Materials and methods

Teeth

This preliminary study involves two human third mandibular molar teeth from the crypt of Santa Maria Maggiore in Vercelli.

The Cathedral of Santa Maria Maggiore, constructed in the 18th century to replace the nearby ‘Santissima Trinità’ church (Tibaldeschi, 1996), features a hypogeal cemetery that served for new interments and the relocation of remains from the former episcopal complex (Fusco et al., 2023; Tibaldeschi, 1996; Vanni et al., 2024). This vaulted subterranean space houses two underground ossuaries. The materials analysed in this study originate from the first ossuary, known as “Hypogeum 1”, currently undergoing archaeological and anthropological investigation. Situated approximately 5 meters below the floor level of the crypt, this subterranean area has been divided into square sectors, each identified by a combination of numbers (1 to 6) and letters (A to F). Furthermore, the square sectors have also been divided in four corners (North-East, North-West, South-East, South-West) facilitating systematic exploration and analysis.

The mandibles selected for examination were chosen from the osteological remains recovered to date, based on the presence of third molars in their original positions. Following identification of the mandibles, the integrity of the third molars was carefully assessed. Selection criteria excluded molars showing macroscopic signs of cracks or fractures.

Ultimately, two mandibles were chosen: one from quadrant 2B Stratigraphic Unit 1 North-East corner (VC SMM24 2B US1 NE), and another from quadrant 2D Stratigraphic Unit 1 South-East corner (VC SMM24 2D US1 SE). From mandible VC SMM24 2B US1 NE a right third molar was extracted (tooth 2B). From mandible VC SMM24 2D US1 SE a left third molar was extracted (tooth 2D).

Before proceeding with the extraction of the selected third molars, the mandibles were photographed in superior, frontal and lateral views. The photographs were acquired with a Nikon D300S camera and lenses AF S Nikkor 18–200mm f/3.5–5.6GII ED and AF S Micro Nikkor 60mm f/2.8 G ED. Two series of

photos were acquired: the first one with metric reference and X-Rite Pantone ColorChecker Classic Mini MSCCMN-RET with chip area of 57 x 86 mm with 24 natural object, chromatic, primary and gray scale colours.

The extraction process was conducted with utmost care using gloves to preserve the integrity of the mandibles. Upon extraction, each tooth was catalogued and securely stored in designated bags, labelled to ensure accurate documentation and preservation. After the extraction, the teeth were also photographed in occlusal, lingual, buccal, mesial, and distal views with the same instrumentation and procedure.

The tooth from VC SMM24 2B US1 NE (Figure 1), from now on tooth 2B, exhibited two well-formed roots and a naturally worn occlusal surface.

There was a slight tartar deposit observed on both the lingual and buccal surfaces. Additionally, a small penetrating buccal root cavity was noted (Rose and Ungar, 1998). Tooth 2D (Figure 2) presented with two roots that were strongly curved distally. The occlusal surface did not show significant wear, and all four cusps were still discernible. Additionally, there were no signs of tartar, only a non-penetrating occlusal cavity was evident (Rose & Ungar, 1998). The teeth were complete and did not present significant anomalies or pathologies, so they met the criteria stated in the technical protocol for digital acquire.

The teeth were measured with a Mitutoyo 500-181-30, ABS AOS digital metric caliper with a range of 0-150 mm and a sensitivity of 0.01 mm without data output and an accuracy of 0.5 mm. Each

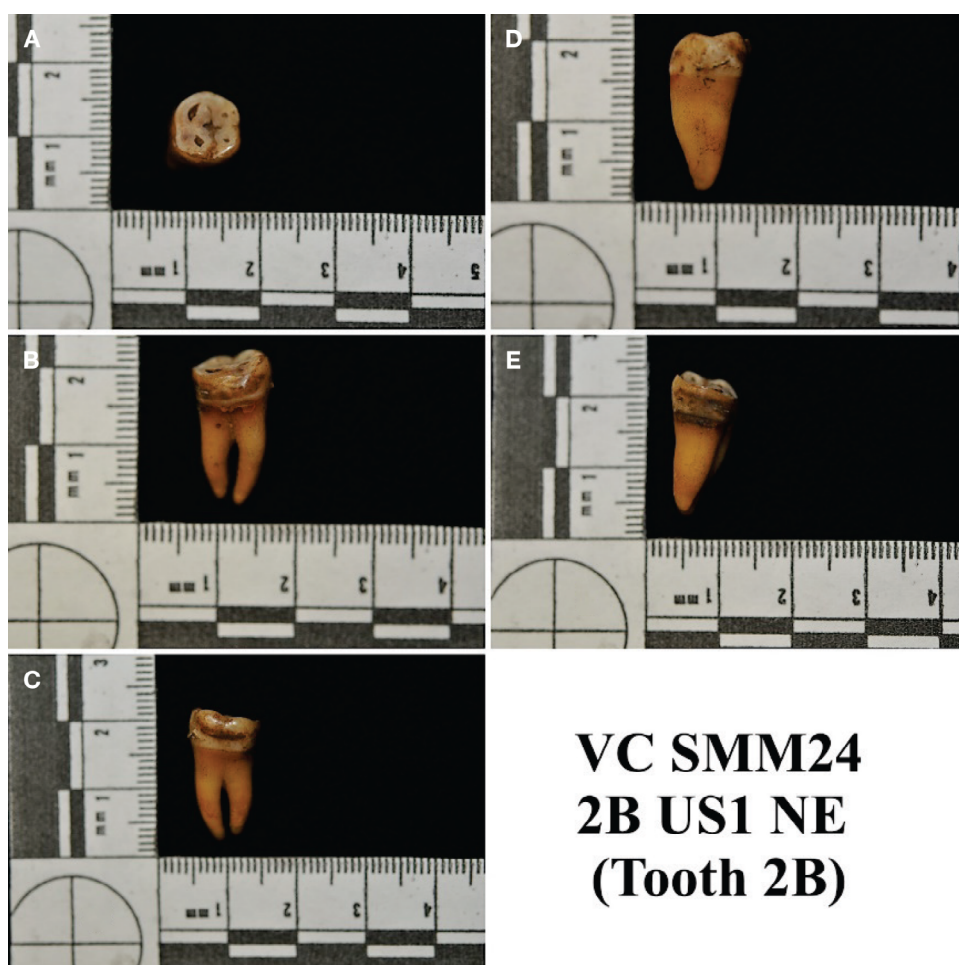


Figure 1. Tooth 2B (a: occlusal norm, b: buccal norm, c: lingual norm, d: mesial norm, e: distal norm).

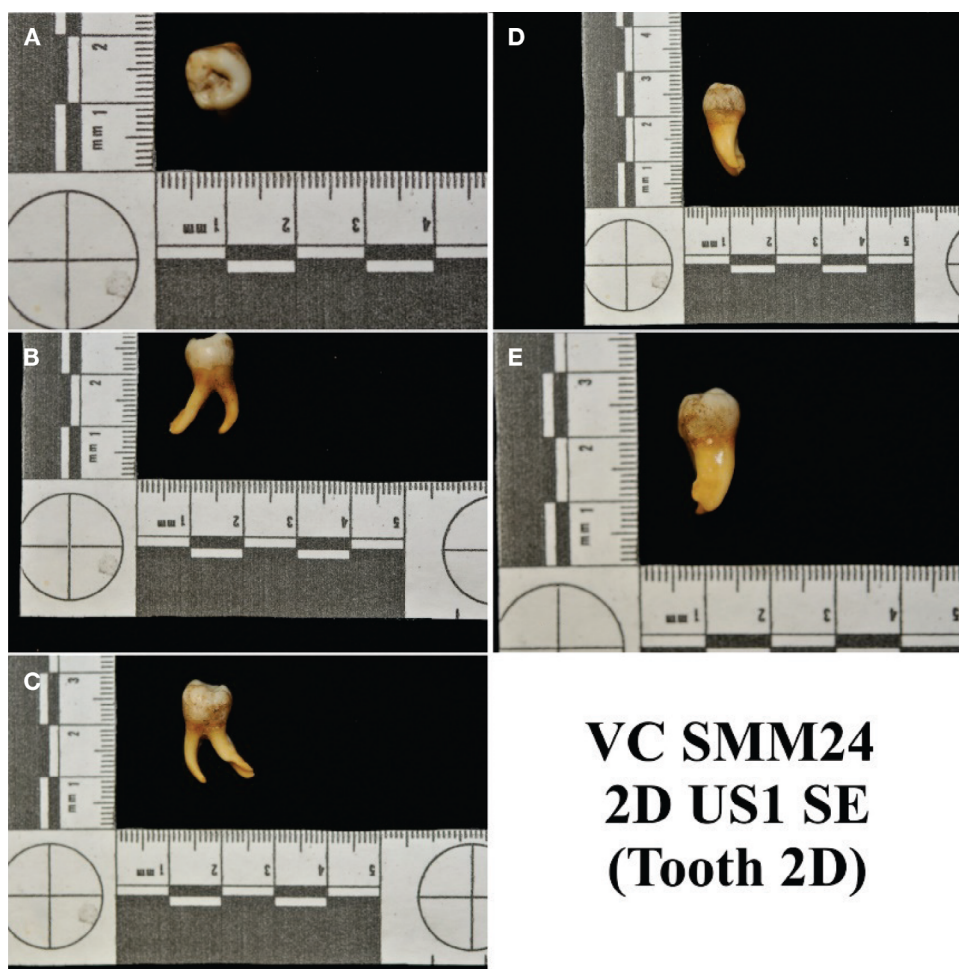


Figure 2. Tooth 2D (a: occlusal norm, b: buccal norm, c: lingual norm, d: mesial norm, e: distal norm).

tooth was measured 3 times by one expert on the total maximal length, the mesio-distal diameter and the bucco-lingual diameter. Mean and standard deviation were calculated for each measurement.

To eliminate any distortion provided by the measurement unit, the data are normalized according to the greatest measure, specifically total length: total length, bucco-lingual diameter and mesio-distal diameter are then divided by the total length.

Digital acquire and IUD processing

The scanning is performed with the structured light scanner SHINING 3D EinScan-SP V1. It is a desktop structured light scanner, suitable for small objects. The scanner has a single shot accuracy lower than

0.5 mm, with point distance between 0.17 and 0.2 mm. The scan volume, using the turntable, should not be lower than 30 x 30 x 30 mm or greater than 200 x 200 x 200 mm. The scanner is composed of two inclined cameras with a resolution of 1.3 Mega Pixels at a certified distance from the white LED light source. The source of light projects different patterns on the object surface from which range images are obtained. The stand-off distance is between 290 and 480 mm.

The scanner requires at least that the operative system is Microsoft Windows 7, Nvidia graphic card with memory greater than 1 GB, a dual-core i5 CPU or higher 8 GB of memory and one serial connector USB 2.0 or 3.0.

The processing has been performed with a computer HP Zbook 15u G6 (version SBKPF, serial

number 5CG9377GJH) with Intel Core i5-8265U CPU 1.60GHz (6 MB cache, 4 cores, 8 threads) as a CPU, a 4 GB AMD Radeon Pro WX3200 (Polaris 12) graphic card and a 1 GB Intel UHD Graphics 620 (Whiskey Lake-U GT2) [Hewlett-Packard] graphic card. The operating system is Microsoft Windows 11 Professional (x64) Build 22631.3737 (23H2) and the storage is a 512 GB SAMSUNG MZVLB512HAJQ-000H1. The workstation is provided with two USB 3.1 serial connectors.

The scanner is set up differently from the producer's suggestions to optimize the configuration for the scanning of teeth and to lower the minimal acquisition volume. The scanner is rotated of 60° down on the line connecting the two cameras and positioned at a height of 26,6 cm: this configuration is based on a preliminary evaluation, resulting from the observation of the obtained point clouds. The turntable is positioned at a distance of 38 cm from projector using a dedicated PVC bar. The tooth is positioned on the turntable with coded targets.

To ensure stability, the scanner is mounted on a self 3D printed trestle. The project is a Free Libre (EUPL 1.2) model build by FreeCAD 0.21.1 software and printed with Creality K1C printer. The material used is Creality Hyper PLA with Carbonium 1,75 mm.

The alignment is performed with the ExScan S 3.13 software. The following settings are used: "turntable with coded targets" as align mode and 18 steps (one every 20°) with the HDR light option enabled. The speed was set to 5 to avoid image blurring and to ensure the stability of the tooth. On each tooth 3 partial digital acquire are performed in the following order:

- occlusal surface of the tooth facing downwards, with the buccal surface facing the scanner head;
- tooth resting on the lingual surface and the occlusal surface oriented towards the scanner head;
- tooth resting on the lingual surface and the occlusal surface oriented towards the scanner head.

For the first partial acquire a base made of STAEDTLER modelling clay BLAU 8421-37 is required to keep the tooth in place (Figure 3). The base is enveloped in a plastic film to avoid alteration of the tooth. This process is based on a preliminary evaluation.

For each partial digital acquire, scanner settings, date, starting time and ending time were registered with the number of points for each partial acquire. The total amount of points was also registered.

For each tooth one complete scanning was done using the technical protocol described.

The obtained point cloud is exported in ASCII XYZN format with the predefined scale of point distance of 1mm. This step is fundamental to import the point cloud into the *osteo_labdig* software. It is written in Python version 3.10.5 with the Open3D module version 0.18.0 and numpy 1.25.2.

After importing the point cloud, the point cloud normals are recalculated and normalized, the point cloud center is translated to the origin and duplicated points are removed (*Ostéo_labdig/Sources/Cgui/Cgui.Py at Master · Labdig3a/Ostéo_labdig · GitHub*, n.d.).

The algorithm used to extract the indexes on the point cloud is the function `get_oriented_bounding_box()` from the Python API of the library Open3D (*Open3D - Docs - Python API (Geometry, Point Cloud)*, n.d.; *Open3D/Cpp/Open3d/Geometry/BoundingBoxVolume.Cpp at Main · Is-Org/Open3D*, n.d., ll. 134–188). The library Open3D was chosen because it offers both an integrated GUI (Graphical User Interface) and the possibility to perform massive data analysis through scripts.

For the execution of the algorithm, a custom workstation mounted by the company *progettosl - LEICON* of Serenella Saccon was used, with the mainboard Asus ROG STRIX B460-F Gaming, CPU Intel Core i9-10900F Comet Lake, 64GB of RAM, graphic card NVIDIA GeForce RTX 3060 12GB and SSD WD Blue SA510 1000GB.

The algorithm calculates the convex hull of the point cloud, which is the smallest convex polygon that encompasses all the points in the point cloud, including the boundary. With the point cloud obtained with the convex hull, mean and covariance are calculated. This allows to compute a PCA (Principal Component Analysis), a technique taken from multivariate statistics which defines an orthogonal transformation to a diagonal covariance matrix from an existing dataset (Denis, 2021, p. 424). In other words, Principal Component Analysis is a statistical method employed to reduce the dimensionality of a dataset while preserving

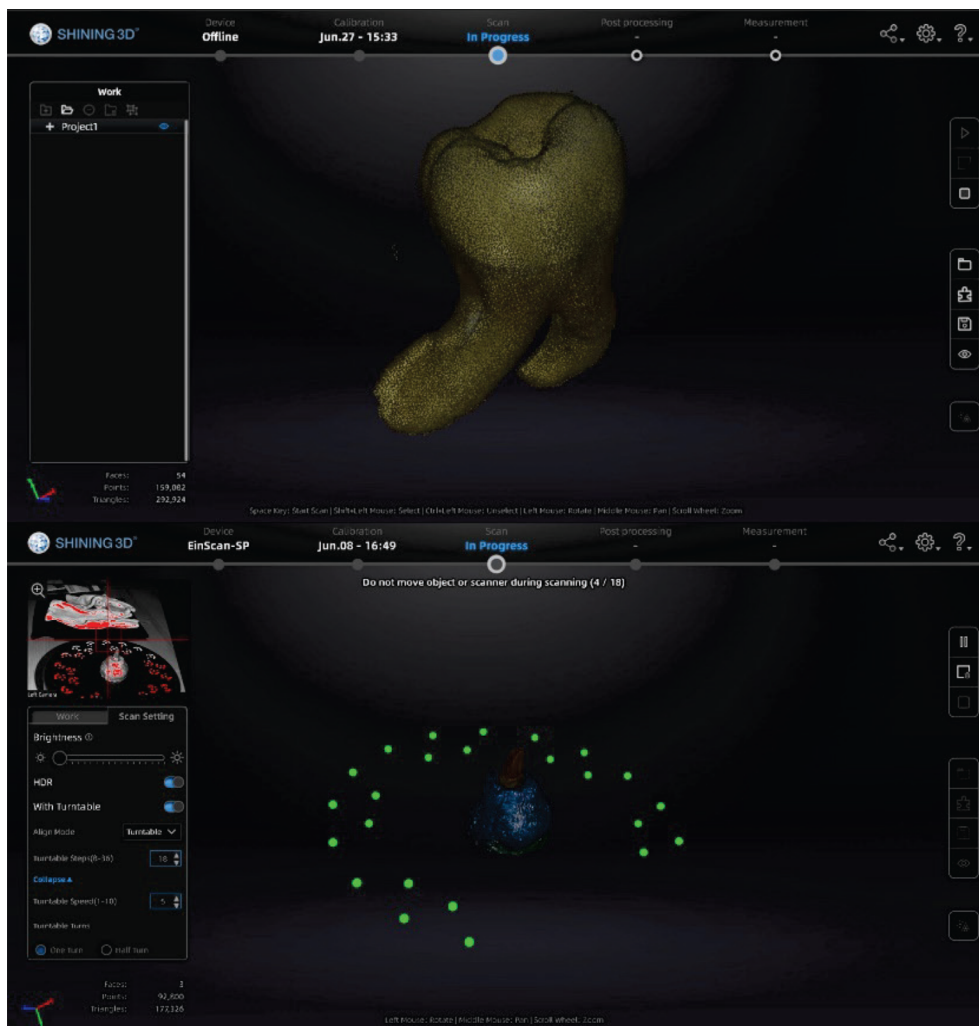


Figure 3. Point cloud of tooth 2D from the software ExScan S. Above the complete cloud, below a stage of the first partial acquisition.

the majority of its variability. This is accomplished by transforming the data into a new set of uncorrelated variables, known as principal components, which are ranked according to the variance they capture. PCA is extensively utilized for noise reduction, feature extraction, and data visualization across diverse fields, including biological anthropology, thereby facilitating the analysis and interpretation of complex data (Kassambara, 2017, p. 170). In this case, a PCA was performed on the point cloud to reorient the axes according to the point distribution. This is done by calculating the mean vector and the covariance matrix of the point cloud.

The covariance matrix is used to compute the eigenvectors and eigenvalues through an instance of the class `Eigen::SelfAdjointEigenSolver`, which exploits the fact that the matrix is selfadjoint to obtain a more accurate and faster response (*Eigen::SelfAdjointEigenSolver< MatrixType_ > Class Template Reference*, n.d.). The eigenvectors are then reordered in a descending manner, to ensure correct alignment, and then normalized.

The convex hull is then transformed into the local coordinate system, an Axis Aligned Bounding Box is calculated and the centre, rotation and extent of this bounding box are passed to the empty

OrientedBoundingBox (OBB) object created inside the function.

The algorithm was applied at different voxel values (None, 0.1, 1, 10) in order to verify the independence from the number of points composing the convex hulls and after a rotation of 45° on the three axes, to verify the rotation invariance. The values were rounded at the 7th decimal digit with the function `numpy.round()` to eliminate the digits varying due to the hardware limits in processing floating point numbers.

To eliminate any distortion provided by the measurement unit and scale, the data are normalized according to the greatest measure, specifically `ext_0`: `ext_0`, `ext_1` and `ext_2` are then divided by `ext_0`. The normalization of the point cloud extension indexes, as it is calculated here, brings to the definition of a new object that we defined as NOOBB (Normalized Osteological Oriented Bounding Box).

Results

Tooth 2B was acquired in 38 minutes with data registration (35 minutes for the acquisition alone). The

point cloud is composed of 163520 points (Figure 4). The scanning was roughly evaluated by an operator by sight and it showed a high correspondence with the object with respect to the geometry. In Tables 1, 2 and 3 the data about tooth measures and indexes are provided.

Tooth 2D was acquired in 40 minutes with data registration (34 minutes for the acquisition alone). The point cloud is composed of 159082 points (Figure 5). The scanning was roughly evaluated by an operator by sight and it showed a high correspondence with the object with respect to the geometry. In Tables 4, 5 and 6 the data about tooth measures and indexes are provided.

Discussion

The development of a verification and acquisition technical protocol commence by testing and detecting the limits of the instrumentation: the reduced dimensions and the relatively complex shape of human teeth are a good example of how the limits of the scanner EinScan-SP V1 are evaluated. However,

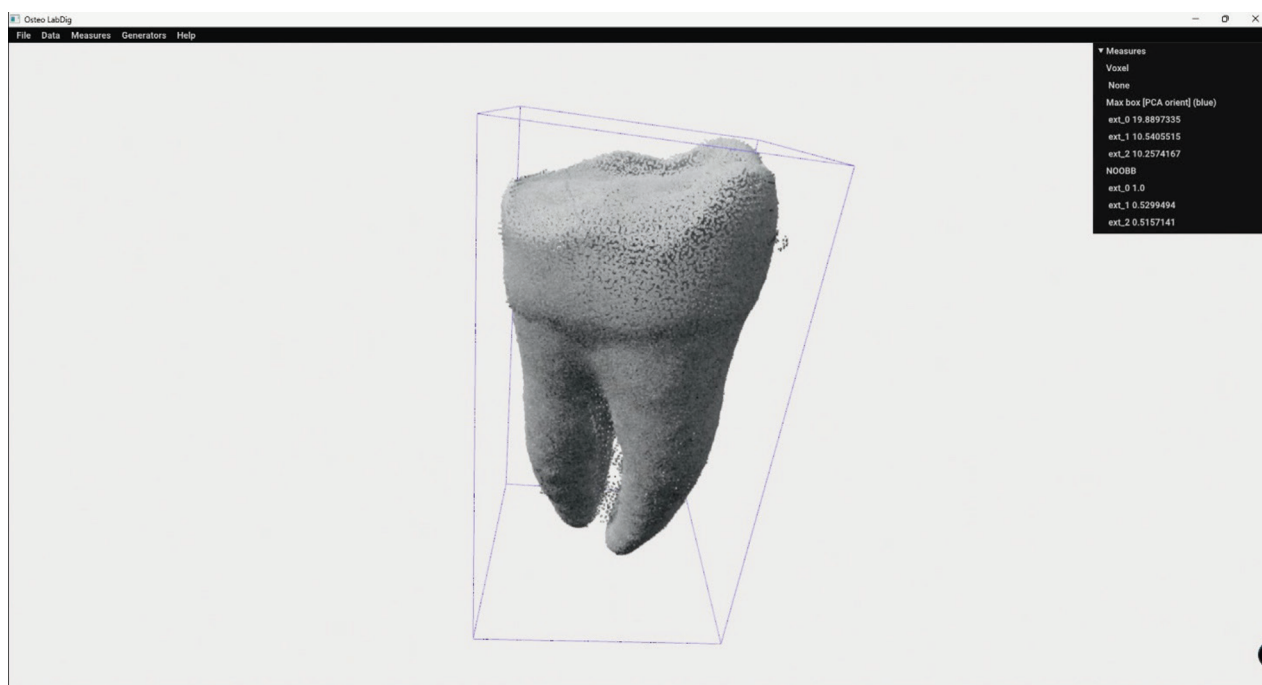


Figure 4. Point cloud of tooth 2B from the software `osteo_labdig`. On the right voxel settings, OBB (Max bound [PCA orient]) and NOOBB index.

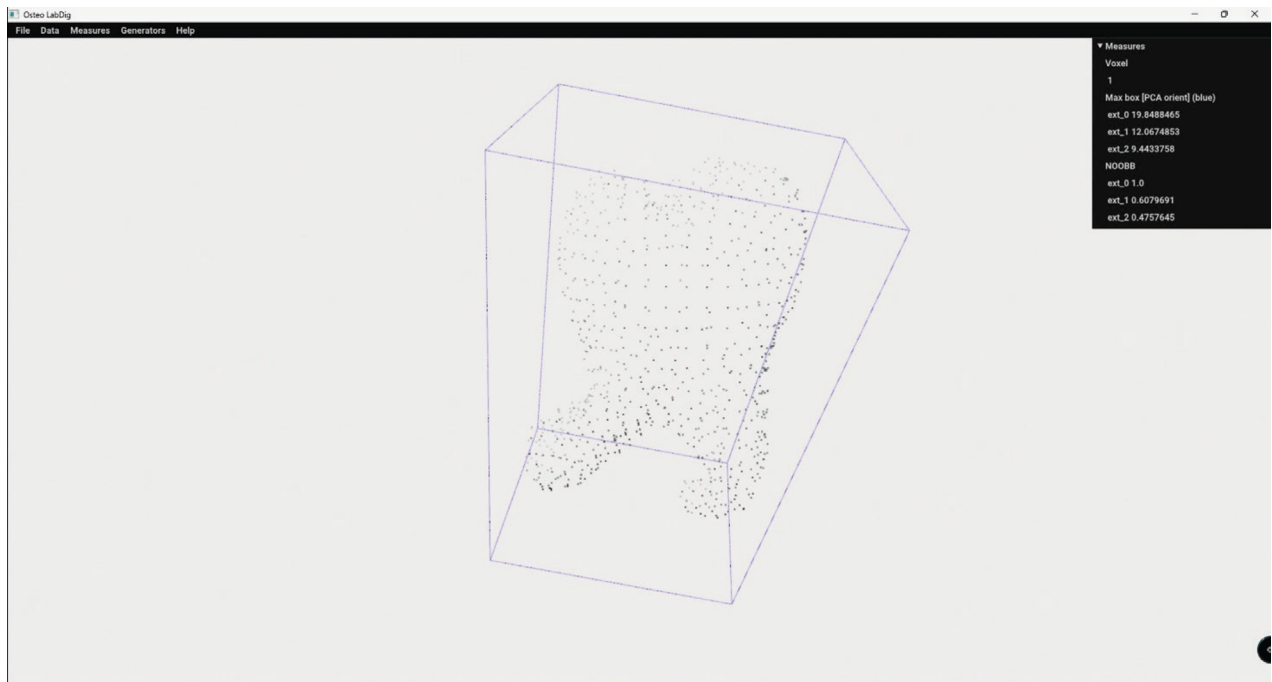


Figure 5. Point cloud of tooth 2D from the software osteo_labdig. On the right voxel settings, OBB (Max bound [PCA orient]) and NOOBB index.

Table 1. Measures taken on tooth 2B.

| Measure | Mean (mm) | Sample standard deviation (mm) |
|------------------------|-----------|--------------------------------|
| Total length | 19.12 | 0.49 |
| Bucco-lingual diameter | 9.45 | 0.07 |
| Mesio-distal diameter | 10.24 | 0.02 |

Table 2. Measures taken on tooth 2B normalized according to the total length.

| Measure | Normalized means | Uncertainty |
|------------------------|------------------|-------------|
| Total length | 1 | 0.0006568 |
| Bucco-lingual diameter | 0.4942469 | 0.0001759 |
| Mesio-distal diameter | 0.5355649 | 0.0001769 |

the acquisitions presented here are only the beginning of the research: more test must be performed to assess and verify the repeatability and reproducibility of the digital acquire, possibly using different scanners with the same hardware and software characteristics. Angles, heights and environmental conditions will be

systematically tested with a well established experimental protocol. This is particularly important for low cost instrumentation, because of the lower stability and potentially higher SNR (Signal-to-Noise Ratio).

The scanner configuration used to acquire was assessed by means of qualitative evaluation of the acquired point cloud with respect to the object and should confirmed or modified performing the aforementioned tests and a quantitative evaluation of the point cloud on multiple acquisitions. This can be done in statistical terms, after a careful evaluation of the alignment algorithms.

Calculations on the point cloud are performed in a digital environment, which is by no means similar to the physical world: to conceptualize this difference, the IUD is defined, an environment where only points exist, with its own rules and characteristics. It is possible to interact with this digital environment and perform calculations on the point cloud using a software. For anthropology, the FLOSS (Free Libre and Open Source) software osteo_labdig is presented.

Indexes on the point cloud are obtained by the `get_oriented_bounding_box()` function from the Open3D library. OBB is an algorithm mainly developed for

Table 3. Extension indexes in relation with voxel and rotation of tooth 2B.

| Algorithm | Extension | Not rotated | | | | Rotated |
|-----------|-----------|-------------|------------|------------|------------|------------|
| | | Voxel | | | | Voxel |
| | | None | 0.1 | 1 | 10 | None |
| NOOBB | ext_0 | 1 | 1 | 1 | 1 | 1 |
| | ext_1 | 0.5299494 | 0.5566535 | 0.5331996 | 0.5298938 | 0.5299494 |
| | ext_2 | 0.5157141 | 0.4901226 | 0.4799575 | 0.4737693 | 0.5157141 |
| OBB | ext_0 | 19.8897335 | 19.8794592 | 19.6615002 | 14.7895136 | 19.887335 |
| | ext_1 | 10.5405515 | 11.0659711 | 10.4835035 | 7.8368716 | 10.5405515 |
| | ext_2 | 10.2574167 | 9.7433722 | 9.436685 | 7.0068172 | 10.2574167 |

Table 4. Measures taken on tooth 2D.

| Measure | Mean (mm) | Sample standard deviation (mm) |
|------------------------|-----------|--------------------------------|
| Total length | 19.66 | 1.09 |
| Bucco-lingual diameter | 9.6 | 0.14 |
| Mesio-distal diameter | 9.57 | 0.02 |

Table 5. Measures taken on tooth 2D normalized according to the total length.

| Measure | Normalized means | Uncertainty |
|------------------------|------------------|-------------|
| Total length | 1 | 0.0030739 |
| Bucco-lingual diameter | 0.9375 | 0.0015406 |
| Mesio-distal diameter | 0.9345703 | 0.0014384 |

computer vision and videogame development (Ericson, 2004, pp. 101–112), but it is ultimately a dimensional and shape descriptor: this justifies its use in the IUD environment for anthropology. Ericson warns about the risk of using PCA-based OBB algorithms if internal points are present and about their effect on the orientation of OBB (Ericson, 2004, p. 108). This risk is avoided by means of the convex hull, which excludes internal points from the calculation.

As showed in tables 3 and 6, being PCA-based, the algorithm is also invariant to point cloud orientation,

whereas it is affected by the voxelization, probably because of the change in the convex hull geometry. Voxelization is a downsampling procedure which has the advantage to reduce the amount of data and affords to execute the algorithm on less performant workstations, but by now no solution has been found to the problems related to detail loss (Lyu et al., 2024). This is anyway a good exemplification of how IUD rules and indexes are by no means comparable to the measures taken on the physical objects.

To reduce the scale effect of the extension values a normalization of the OBB indexes has been performed, dividing all the three indexes by the largest, which is ext_0: this defines a new object which we decided to call NOOBB (Normalized Osteological Oriented Bounding Box). Additional studies should and will be carried out on known samples to verify if there is any correlation between these indexes and sex, age or other aspects of the biological profile.

Conclusions

In conclusion, this preliminary work commence to define a technical protocol for the digital acquire of human mandibular third molars to obtain accurate point clouds, conceptualizes the IUD, the digital environment in which point cloud processing is carried out, and presents the software `osteo_labdig`, aimed to perform point cloud processing for osteological data through the libraries `Open3D` and `Numpy`.

Table 6. Extension indexes in relation with voxel and rotation of tooth 2D.

| Algorithm | Extension | Not rotated | | | | Rotated |
|-----------|-----------|-------------|------------|------------|------------|------------|
| | | Voxel | | | | Voxel |
| | | None | 0.1 | 1 | 10 | None |
| NOOBB | ext_0 | 1 | 1 | 1 | 1 | 1 |
| | ext_1 | 0.6305848 | 0.6400005 | 0.6079691 | 0.5328179 | 0.6305848 |
| | ext_2 | 0.4841793 | 0.4827599 | 0.4757645 | 0.3899878 | 0.4841793 |
| OBB | ext_0 | 20.0629733 | 20.0589035 | 19.8488465 | 15.6655379 | 20.0629733 |
| | ext_1 | 12.6514054 | 12.8377085 | 12.0674853 | 8.3468791 | 12.6514054 |
| | ext_2 | 9.7140767 | 9.6836342 | 9.4433758 | 6.1093694 | 9.7140767 |

Acknowledgements: We extend our deepest gratitude to Fondazione Cassa di Risparmio di Torino for their generous financial support of the bioarchaeological project at the Cemetery of Santa Maria Maggiore in Vercelli. The excavations and related research were conducted under the scientific supervision of the Soprintendenza Archeologia Belle Arti e Paesaggio for the Provinces of Biella, Novara, Verbano-Cusio-Ossola, and Vercelli, with invaluable collaboration and assistance from the Ufficio Diocesano per i Beni Culturali Ecclesiastici e l'Edilizia di Culto, Arcidiocesi Vercelli. We also express our gratitude to the communities who developed the FLOSS software we used for their invaluable contribution, without which this manuscript could not be written: the software Libre Office 24.2 with Mozilla Public License (MPL) v 2.0 for the writing, GIMP 2.10.22 for image fixing, ShareX 16.1.0 to capture the screenshots, FreeCAD 0.21.1 with Lesser General Public License version 2 or superior (LGPL2+) and Zotero 6 with the GNU Affero General Public License (version 3) for the reference organization and insertion.

References

- Balletti, C., Bertellini, B., Gottardi, C., & Guerra, F. (2019). Geomatics techniques for the enhancement and preservation of cultural heritage. *The International Archives of the Photogrammetry, Remote Sensing and Spatial Information Sciences, XLII-2/W11*, 133–140. <https://doi.org/10.5194/isprs-archives-XLII-2-W11-133-2019>.
- Bastir, M., García-Martínez, D., Torres-Tamayo, N., Palancar, C. A., Fernández-Pérez, F. J., Riesco-López, A., Osborne-Márquez, P., Ávila, M., & López-Gallo, P. (2019). Workflows in a virtual morphology lab: 3D scanning, measuring, and printing. *Journal of Anthropological Sciences*, 97, 107–134. Scopus. <https://doi.org/10.4436/jass.97003>.
- Colosimo, B. M., Pacella, M., & Senin, N. (2015). Multisensor data fusion via Gaussian process models for dimensional and geometric verification. *Precision Engineering*, 40, 199–213. Scopus. <https://doi.org/10.1016/j.precisioneng.2014.11.011>.
- Denis, D. J. (2021). *Applied univariate, bivariate, and multivariate statistics: Understanding statistics for social and natural scientists, with applications in SPSS and R*. John Wiley & Sons.
- Diara, F. (2023). Structured-Light Scanning and Metrological Analysis for Archaeology: Quality Assessment of Artec 3D Solutions for Cuneiform Tablets. *Heritage*, 6(9), Article 9. <https://doi.org/10.3390/heritage6090317>.
- Dickin, F., Pollard, S., & Adams, G. (2021). Mapping and correcting the distortion of 3D structured light scanners. *Precision Engineering*, 72, 543–555. <https://doi.org/10.1016/j.precisioneng.2021.06.001>.
- Eigen: Eigen::SelfAdjointEigenSolver< MatrixType_ > Class Template Reference.* (n.d.). Retrieved 2 July 2024, from https://eigen.tuxfamily.org/dox/classEigen_1_1SelfAdjointEigenSolver.html
- Ericson, C. (2004). *Real-time collision detection*. Crc Press.
- Evgenikou, V., & Georgopoulos, A. (2015). Investigating 3D reconstruction methods for small artifacts. *ISPRS - International Archives of the Photogrammetry, Remote Sensing and Spatial Information Sciences, XL-5/W4*, 101–108. <https://doi.org/10.5194/isprsarchives-XL-5-W4-101-2015>.
- Fusco, R., Messina, C., Tesi, C., & Vanni, A. (2023). “Capta est ne malitia mutaret intelletum eius...”: Study on a natural mummy from an underground cemetery (18–19th century). *Med. Hist.*, 7, e2023044.
- Garashchenko, Y., Kogan, I., & Rucki, M. (2022). Comparative accuracy analysis of triangulated surface models of a fossil skull digitized with various optic devices. *Metrology and Measurement Systems*, 29(1), Article 1. Scopus. <https://doi.org/10.24425/mms.2022.138547>.
- Georgopoulos, A., Oikonomou, Ch., Adamopoulos, E., & Stathopoulou, E. K. (2016). Evaluating unmanned aerial platforms for cultural heritage large scale mapping. In Remondino F., 3D Optical Metrology FBK Trento via Sommarive 18, 38123, Trento, Rieke-Zapp D., Pavelka K., Hodac J., Shortis M., Halounova L., Rinaudo F., Boehm J., Safar V., & Scaioni M. (Eds.), *Int. Arch. Photogramm., Remote Sens. Spat. Inf. Sci. - ISPRS Arch.* (Vol. 41, pp. 355–362).

- International Society for Photogrammetry and Remote Sensing; Scopus. <https://doi.org/10.5194/isprsarchives-XLI-B5-355-2016>.
- Jacobs, L., Dvorak, J., Cornelius, A., Zamerowski, R., No, T., & Schmitz, T. (2023). Structured light scanning artifact-based performance study. *Manufacturing Letters*, 35, 873–882. <https://doi.org/10.1016/j.mfglet.2023.07.014>.
- Kassambara, A. (2017). *Practical guide to principal component methods in R: PCA, M (CA), FAMD, MFA, HCPC, factoextra* (Vol. 2). Sthda.
- Kusuma Frisky, A. Z., Fajri, A., Brenner, S., & Sablatnig, R. (2020). Acquisition evaluation on outdoor scanning for archaeological artifact digitalization. In Farinella G.M., Radeva P., & Braz J. (Eds.), *VISIGRAPP - Proc. Int. Jt. Conf. Comput. Vis., Imaging Comput. Graph. Theory Appl.* (Vol. 5, pp. 792–799). SciTePress; Scopus. <https://www.scopus.com/inward/record.uri?eid=2-s2.0-85083513105&partnerID=40&md5=b399b8a26b2de81633365079b216a3dd>.
- labdig3a/osteo_labdig: *Digital laboratory for osteological measurements*. (n.d.). Retrieved 2 June 2024, from https://github.com/labdig3a/osteo_labdig.
- Lyu, W., Ke, W., Sheng, H., Ma, X., & Zhang, H. (2024). Dynamic Downsampling Algorithm for 3D Point Cloud Map Based on Voxel Filtering. *Applied Sciences*, 14(8), Article 8. <https://doi.org/10.3390/app14083160>.
- Maté-González, M. Á., Aramendi, J., González-Aguilera, D., & Yravedra, J. (2017). Statistical comparison between low-cost methods for 3D characterization of cut-marks on bones. *Remote Sensing*, 9(9), Article 9. Scopus. <https://doi.org/10.3390/rs9090873>.
- Menna, F., Nocerino, E., Remondino, F., Dellepiane, M., Callieri, M., & Scopigno, R. (2016). *3D Digitization of an heritage masterpiece—A critical analysis on quality assessment*. 41, 675–683. Scopus. <https://doi.org/10.5194/isprsarchives-XLI-B5-675-2016>.
- Morena, S., Barba, S., & Álvaro-Tordesillas, A. (2019). *Shining 3D EinScan-Pro, application and validation in the field of cultural heritage, from the Chillida-Leku museum to the archaeological museum of Sarno*. 42(2/W18), 135–142. Scopus. <https://doi.org/10.5194/isprs-archives-XLII-2-W18-135-2019>.
- Open3D - Docs—Python API (geometry, point cloud). (n.d.). Retrieved 2 June 2024, from https://www.open3d.org/docs/latest/python_api/open3d.geometry.PointCloud.html
- Open3D/cpp/open3d/geometry/BoundingBoxVolume.cpp at main · isl-org/Open3D. (n.d.). GitHub. Retrieved 2 June 2024, from <https://github.com/isl-org/Open3D/blob/main/cpp/open3d/geometry/BoundingBoxVolume.cpp>
- Osteo_labdig/sources/cgui/cgui.py at master · labdig3a/osteo_labdig · GitHub. (n.d.). Retrieved 2 July 2024, from https://github.com/labdig3a/osteo_labdig/blob/master/sources/cgui/cgui.py#L156C1-L209C25
- Plato. (n.d.). *Phaedrus*.
- Rose, J. C., & Ungar, P. S. (1998). Gross dental wear and dental microwear in historical perspective. In *Dental anthropology: Fundamentals, limits and prospects* (pp. 349–386). Springer.
- Russo, M., & Senatore, L. J. (2022). *Low-cost 3d techniques for real sculptural twins in the museum domain*. 48(2/W1-2022), 229–236. Scopus. <https://doi.org/10.5194/isprs-archives-XLVIII-2-W1-2022-229-2022>.
- Tibaldeschi, G. (1996). La Chiesa di S. Maria Maggiore di Vercelli e l'Assunzione di Paolo Borroni. *Bollettino Storico Vercellese*, 2, 131–150.
- Vanni, A., Fusco, R., Tesi, C., & Licata, M. (2024). Autopsy or anatomical dissection? Comparative analysis of an osteoarchaeological sample from an 18-19th century hypogeal cemetery (northern Italy). *Journal of Archaeological Science: Reports*, 54, 104418.
- Weber, G. W. (2014). Another link between archaeology and anthropology: Virtual anthropology. *Digital Applications in Archaeology and Cultural Heritage*, 1(1), Article 1. Scopus. <https://doi.org/10.1016/j.daach.2013.04.001>.
- Williams, R., Thompson, T., Orr, C., & Taylor, G. (2024). Developing a 3D strategy: Pipelines and recommendations for 3D structured light scanning of archaeological artefacts. *Digital Applications in Archaeology and Cultural Heritage*, 33. Scopus. <https://doi.org/10.1016/j.daach.2024.e00338>.
- Zhou, Q.-Y., Park, J., & Koltun, V. (2018). Open3D: A Modern Library for 3D Data Processing. *arXiv:1801.09847*.

Correspondence:

Nicol Rossetti
 Department of Biotechnology and Life Sciences,
 University of Insubria.
 E-mail: nicol.rossetti@uninsubria.it